Optimized Decoupling of Hyperbolic Conservation Laws to Predict High Speed Flow Physics

Noor Fatima Siddiqui[1], Mukkarum Hussain[2], Asif Raza Khan[1]

***Abstract*--Total Variation Diminishing (TVD) schemes are widely used to capture high resolution and non-oscillatory supersonic and hypersonic flow problems. However, discretization and decoupling of the governing equations into nonlinear wave equation induces false numerical dissipation which affects the accuracy of results as well as rate of convergence. This deficiency of TVD schemes can be reduced by an adequate treatment of various parameters that signifies the effect of this dissipation. An appropriate scaling of eigenvectors and eigenvector matrix is one of the strategies to control the amount of numerical dissipation. In present work, hybrid scaling based on some classical scaling factors is proposed and tested on shock tube problem using SOD, Lax and Inverse Shock test cases. Although the computed results are found to be slightly less dissipative in comparison to the scaling used by Hoffmann and Yee, the proposed hybridized scaling and its theoretical aspects on Harten's 2nd order TVD scheme has opened new challenges for the researchers.**

***Keywords*--Numerical Dissipation, Shock waves and Contact, Eigenvectors and Eigenvector Matrix, Shock Tube Problem, TVD scheme, Hypersonic Flow.**

I. INTRODUCTION

Computational Fluid Dynamics (CFD) is a tool to perform fluid flow simulations with computer aid based on numerical solutions of governing equations. Particularly in the area of hypersonic flow applications, CFD is achieving a growing attention of the researchers. The design of high-speed vehicles highly depends on precise predictions of aerothermodynamics, hypersonic flow, high enthalpy fluid dynamics and shock wave boundary layer interactions etc [1-3]. That is why, the growth of accurate numerical techniques is mandatory in order to provide optimal design of hypersonic vehicles. The complexities of the flow phenomena such as shock wave interactions involved in hypersonic and supersonic flows highly demand the formulation of non-oscillatory high-resolution shock capturing schemes.

Higher order accurate non-oscillatory schemes possess false numerical dissipation which makes accurate estimations of hypersonic flow physics quite challenging, typically at higher Mach numbers [2]. The development of a high resolution and low dissipative shock capturing scheme has been a keen interest of researchers from past few decades [4-8].

Date received: 26 June 2020; Accepted: 30 August 2020.
1. University of Karachi, Karachi 75270 Pakistan.
nfsiddiqui@uok.edu.pk

2. Institute of Space Technology, Karachi Pakistan.

Harten's 2nd order accurate explicit total variation diminishing (TVD) scheme proved to be high resolution non-oscillatory for computations of hyperbolic conservation laws. However, it shows false dissipation for strong discontinuities such as contact and shocks [4], which in turn affects both accuracy and efficiency. This incompatibility of TVD scheme to sharply capture discontinuities can be considerably minimized by controlling the affecting parameters involved. One of the primary features to reduce dissipation is the proper selection of characteristic transformation used in TVD scheme by an appropriate scaling of eigenvectors and eigenvector matrix appearing in the numerical flux formulation.

In present work, some classical scaling factors which are previously used by Hoffman [9] and Yee [10] are used to form a hybrid scaling factor. The scaling factors used in hybridization are flow dependent, hence they can be changed from one point to another in each cell interface location. A new constant scaling factor is also proposed by normalization of eigenvector matrix. The performance of these scaling factors is investigated by comparing the results with numerical solutions obtained using classical form of these factors. Slight improvement is observed, encouraging enough to design and formulate an optimal hybrid structure of some new scaling factors.

II. NUMERICAL METHOD

In this paper, the conservative form of 1D transient Euler equation is used:

$$\frac{\partial U}{\partial t} + \frac{\partial F}{\partial x} = 0 \tag{1}$$

where, the vectors of conserved quantities U and the physical flux F are given in equation 2.

$$U = \begin{bmatrix} \rho \\ \rho u \\ \rho E \end{bmatrix} \quad \text{and} \quad F = \begin{bmatrix} \rho u \\ \rho u^2 + p \\ (\rho E + p)u \end{bmatrix} \tag{2}$$

Nonlinear flux form can be changed into primitive form as,

$$\frac{\partial U}{\partial t} + A\frac{\partial U}{\partial x} = 0 \tag{3}$$

The Jacobian matrix A can be calculated on previous time step and hence primitive form can be treated as linear system of equation, where the Jacobian matrix A of the flux F is defined as:

$$A = \frac{\partial F}{\partial U} = \begin{bmatrix} 0 & 1 & 0 \\ (\gamma-3)\frac{u^2}{2} & (3-\gamma)u & (\gamma-1) \\ (\gamma-1)u^3 - \gamma u E & -\frac{3}{2}(\gamma-1)u^2 + \gamma E & \gamma u \end{bmatrix} \quad (4)$$

Partial differential equation given in (1) can be discretized in terms of numerical flux form as given in equation 5:

$$U_i^{n+1} = U_i^n - \lambda\left(f_{i+\frac{1}{2}}^n - f_{i-\frac{1}{2}}^n\right)\ ;\ \lambda = \frac{\Delta t}{\Delta x} \quad (5)$$

The numerical flux for Harten’s 2nd order explicit TVD scheme is given by equation 6:

$$f_{i+\frac{1}{2}}^n = \frac{1}{2}(F_{i+1} + F_i) + \frac{1}{2\lambda}\sum_{k=1}^{m} R_{i+\frac{1}{2}}^k\Big[g_{i+1}^k + g_i^k - Q^k(\nu_{i+\frac{1}{2}}^k + \gamma_{i+\frac{1}{2}}^k)\alpha_{i+\frac{1}{2}}^k\Big] \quad (6)$$

where,

$$\nu_{i+\frac{1}{2}}^k = \lambda a_{i+\frac{1}{2}}^k \quad (7)$$

and $a = u - c,\ u,\ u + c$ are three real and distinct eigenvalues of the Jacobian matrix A which makes the system strictly hyperbolic, hence ensure the existence of three linearly independent eigenvectors. Physically, these values represent the speed at which information propagates in time marching direction [9,11].

$$\alpha_{i+\frac{1}{2}}^k = R_{i+\frac{1}{2}}^{-1}\Delta_{i+\frac{1}{2}}U \quad (8)$$

$$Q(\nu) = \begin{cases} \frac{\nu^2}{4\epsilon} + \epsilon, & |\nu| < 2\epsilon \\ |\nu|, & |\nu| \geq 2\epsilon \end{cases} \quad (9a)$$

where ϵ is the variable entropy fixing parameter and is calculated by equation 9b [12,13],

$$\epsilon = \varepsilon(|u| + c) \quad (9b)$$

ε is arbitrary constant and is currently taken as 0.1

$$\gamma_{i+\frac{1}{2}}^k = \begin{cases} \frac{g_{i+1}^k - g_i^k}{\alpha_{i+\frac{1}{2}}^k}, & \alpha_{i+\frac{1}{2}}^k \neq 0 \\ 0, & \alpha_{i+\frac{1}{2}}^k = 0 \end{cases} \quad (10)$$

The eigenvector matrix used in the present study is given in equation (11).

$$R = \begin{bmatrix} \beta_1 & \beta_2 & \beta_3 \\ \beta_1(u-c) & \beta_2 u & \beta_3(u+c) \\ \beta_1\left(\frac{u^2}{2} - uc + \frac{c^2}{\gamma-1}\right) & \beta_2\left(\frac{u^2}{2}\right) & \beta_3\left(\frac{u^2}{2} + uc + \frac{c^2}{\gamma-1}\right) \end{bmatrix} \quad (11)$$

and its corresponding inverse is as given in equation 12,

$$R^{-1} = \begin{bmatrix} \frac{u}{4c^2\beta_1}\{2c + u(\gamma-1)\} & -\frac{1}{2c^2\beta_1}\{c + u(\gamma-1)\} & \frac{\gamma-1}{2c^2\beta_1} \\ \frac{1}{\beta_2} - \frac{u^2(\gamma-1)}{2c^2\beta_2} & \frac{u}{c^2\beta_2}(\gamma-1) & -\frac{(\gamma-1)}{c^2\beta_2} \\ -\frac{u}{4c^2\beta_3}\{2c - u(\gamma-1)\} & \frac{1}{2c^2\beta_3}\{c - u(\gamma-1)\} & \frac{\gamma-1}{2c^2\beta_3} \end{bmatrix} \quad (12)$$

where β_1, β_2 and β_3 are non-zero scaling factors of eigenvectors and eigenvector matrix.

Let $B = (\beta_1, \beta_2, \beta_3)$ be the vector whose components are the scaling factors for each column of R in (11).

The monotonized central (MC) limiter function g_i^k used in present study is given in equation 13:

$$g_i^k = S.\max\left(0, \min\left(2\left|\tilde{g}_{i+\frac{1}{2}}^k\right|, S.\tilde{g}_{i-\frac{1}{2}}^k\right), \min\left(\left|\tilde{g}_{i+\frac{1}{2}}^k\right|, 2S.\tilde{g}_{i-\frac{1}{2}}^k\right)\right) \quad (13)$$

where,

$$\tilde{g}_{i+\frac{1}{2}}^k = \frac{1}{2}\left\{Q\left(\nu_{i+\frac{1}{2}}^k\right) - \left(\nu_{i+\frac{1}{2}}^k\right)^2\right\}\alpha_{i+\frac{1}{2}}^k \quad (14)$$

Though the limiter may not need to be same for each field but in order to study the sole effect of proposed scaling factors it is kept same for all characteristic fields.

A. Proposed Scaling Factors

The characteristic fields for the given hyperbolic system comprise of two nonlinear fields corresponding to the eigenvalues $u \pm c$ and a linear field corresponding to eigenvalue u [14-16]. The contact discontinuities are associated with the linear field whereas the expansion fan and shocks are affected by the two distinct nonlinear fields. It is observed that dissipation is unaffected by multiplying scaling factor used by Hoffman (i.e. $\frac{\rho}{c\sqrt{2}}$) and Yee (i.e. $\frac{1}{c^2}$) with the eigenvector associated to a linear filed. This is the reason that scaling is mostly used for nonlinear fields only, whereas for linear field it is taken as unity.

Analysis of TVD schemes using Hoffman’s and Yee’s scaling of eigenvector matrix used in characteristic transformation showed that Hoffman’s scaling factor is more likely suitable to capture expansion fan and Yee’s scaling factor can be considered for better results in shock region [17]. However, the effect of these two scaling parameters is distributed equally at contact. This led to the idea of introducing a hybrid scaling factor which can contribute the features of both parameters in order to improve the accuracy and reducing numerical dissipation in TVD scheme.

In present work, the hybridization of scaling factors is performed by taking the combination of scaling factors used by both Hoffman and Yee [9] [10] as:

$$B_1 = (\beta_1, \beta_2, \beta_3) = \left(\frac{\rho}{c\sqrt{2}}, 1, \frac{1}{c^2}\right) \quad (15)$$

where,

$c_{i+\frac{1}{2}}^2$ is replaced by $\max\left(c_{i+\frac{1}{2}}^2, \min(c_i^2, c_{i+1}^2)\right)$

i.e $\beta_3 = 1/\max\left(c_{i+\frac{1}{2}}^2, \min(c_i^2, c_{i+1}^2)\right)$

The effect of this scaling is analyzed comparing the results with the computations obtained by using each individual scaling factor as given by Hoffman and Yee respectively. Since β_1 and β_3 depends on local density and speed of sound therefore they can vary at each cell location.

Another scaling factor based on the concept of normalizing eigenvector matrix R present in (11) is proposed as $\beta = 2(\gamma - 1)$. Since this factor is independent of the flow variables such as density and velocity therefore it is fixed or constant hence remains same at all grid points. Results computed by using $(\beta_1, \beta_2, \beta_3) = (2(\gamma-1), 1, 2(\gamma-1))$ are converging; however, not so promising in context of numerical dissipation, therefore the existing solutions are compared with another hybridized scaling performed by using Hoffman's and the new scalar as given in equation (16).

$$B_2 = (\beta_1, \beta_2, \beta_3) = \left(\frac{\rho}{c\sqrt{2}}, 1, 2(\gamma - 1)\right) \qquad (16)$$

B. Test Case Description

1D shock tube problem is the one whose analytical solutions are available; therefore, it is used as a test case to investigate the performance of the proposed scaling of eigenvectors and eigenvector matrix. SOD, Lax and Inverse Shock boundary conditions are used as given in Table I. The computational domain is taken as [0,1] with 1000 grid points, setting Courant-Friedrichs-Lewy (CFL) condition equals to 0.8. Initial discontinuity is centered on $x = x_0$ at $t = 0$ and has the following form:

$$U(x,t) = \begin{cases} U_L, & x < x_0 \\ U_R, & x \geq x_0 \end{cases} \qquad (17)$$

where, $x_0 = 0.5$

Simulations of SOD and Lax are carried out up to 0.15 sec whereas for Inverse Shock condition up to 0.05 sec of physical time. All computations are carried out on Intel(R) Core(TM) 2,CPU@2.13 GHz, 5GB RAM.

TABLE I
Boundary Conditions.

	P_R	ρ_R	V_R	P_L	ρ_L	V_L
SOD	0.1	0.125	0.0	1.0	1.0	0.0
LAX	0.571	0.5	0.0	3.528	0.445	0.698
INVERSE SHOCK	1.0	1.0	5.916	29.0	5.0	1.183

III. RESULTS AND DISCUSSION

The effect of proposed hybridized scaling of eigenvectors and eigenvector matrix on dissipation of Harten's 2nd order accurate explicit TVD scheme is analyzed. Results are compared with the consequences of each individual scaling factor to understand the behavior of scheme for capturing expansion fan and discontinuities which are present in high speed flows.

A. Behavior of TVD scheme with $\boldsymbol{B_1}$

Fig 1 to 3 show result at contact discontinuity for the case of SOD, Lax and Inverse Shock boundary conditions respectively computed with B_1 given in equation (15), and the scaling suggested by Hoffman and Yee. In case of SOD, B_1 is found to be good on average in comparison to Hoffman's scaling factor

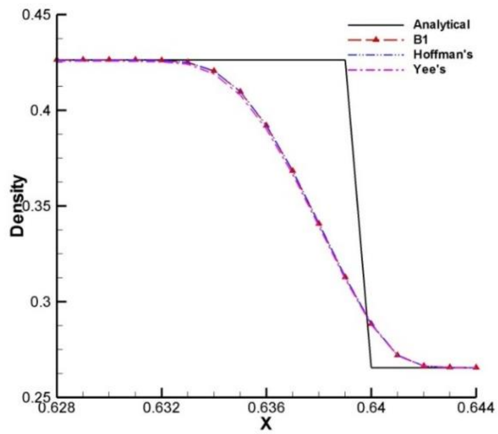

Fig 1: Contact for SOD case with B_1

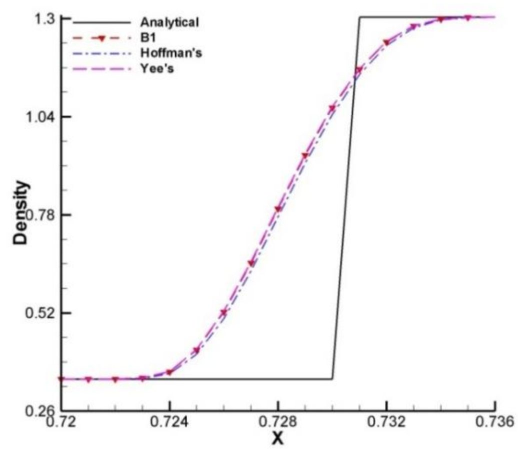

Fig 2: Contact for Lax case with B_1

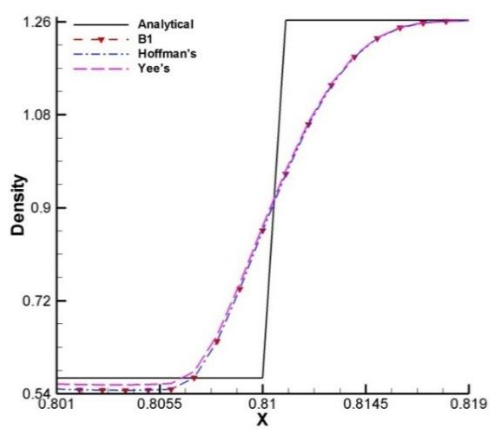

Fig 3: Contact for Inverse Shock case with B_1

(β_1 in B_1) and Yee's scaling factor (β_3 in B_1) for expansion fan, contact is precisely captured by both β_1 and B_1 whereas β_1 is leading in shock region as shown in Fig 4.

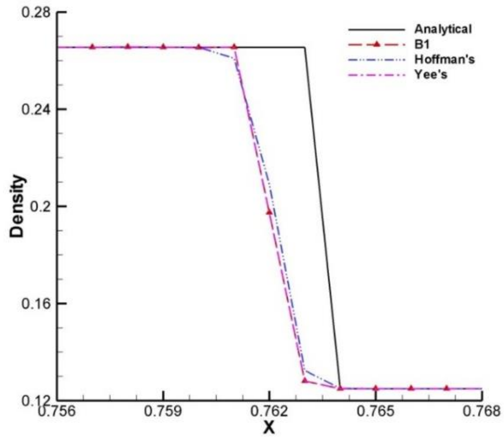

Fig 4: Shock for SOD case with B_1

In order to examine the accuracy of each scaling factor in SOD test case, error analysis for contact discontinuity and shock is also presented in Fig 5 and 6 respectively.

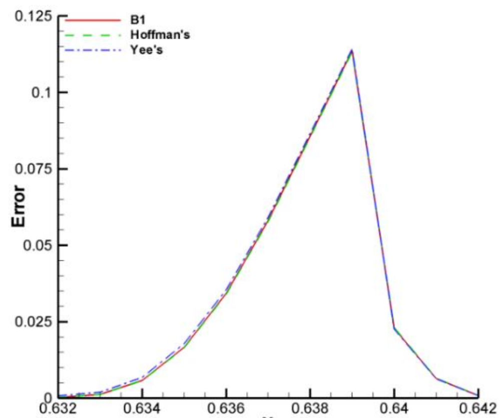

Fig 5: Error analysis for contact in case of SOD with B_1

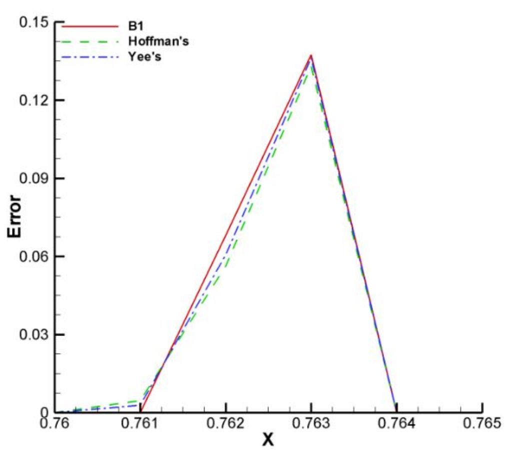

Fig 6: Error analysis for shock in case of SOD with B_1

For test case of Lax, B_1 is observed to be a compromise between β_1 and β_3 for expansion fan as well as for shock. Fig 7 shows the comparison of scaling factors for shock region in Lax case, β_1 is found to give at most 15% less error than B_1 on average and B_1 is approximately 3% improved than β_3 as shown in Fig 8.

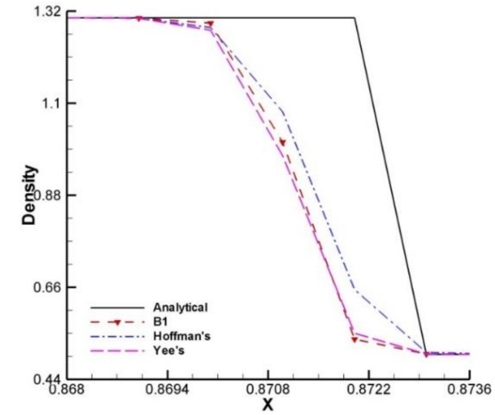

Fig 7: Shock for Lax case with B_1

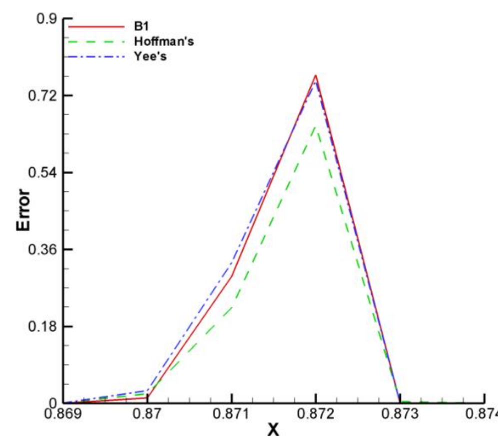

Fig 8: Error analysis for shock in case of Lax with B_1

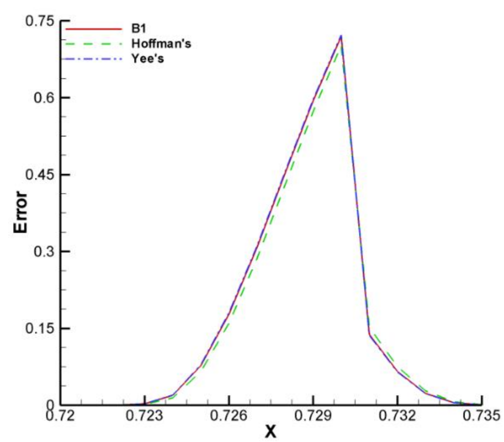

Fig 9: Error analysis for contact in case of Lax with B_1

Results of B_1 and β_3 are almost similar for contact discontinuity, whereas results of β_1 are varying by 2% on average as shown in Fig 9. Fig 10 depicts that the performance of TVD scheme is improved for shock capturing with B_1 in case of Inverse Shock. Computed results with β_1 and B_1 are close to each other for contact as well as expansion fan. Fig 11 and 12 show error estimation at contact and shock locations respectively for Inverse Shock test case.

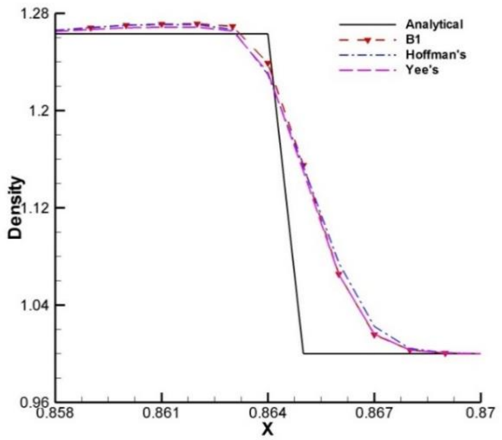

Fig 10: Shock for Inverse Shock case with B_1

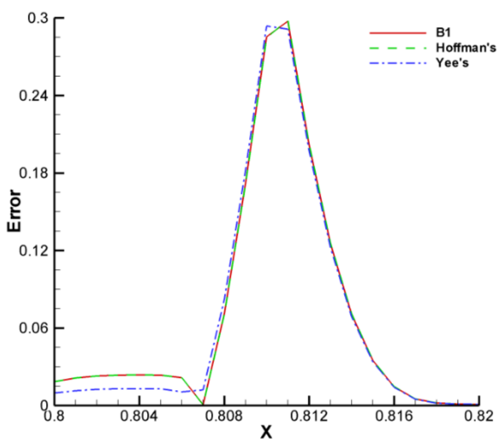

Fig 11: Error analysis for contact in case of Inverse Shock with B_1

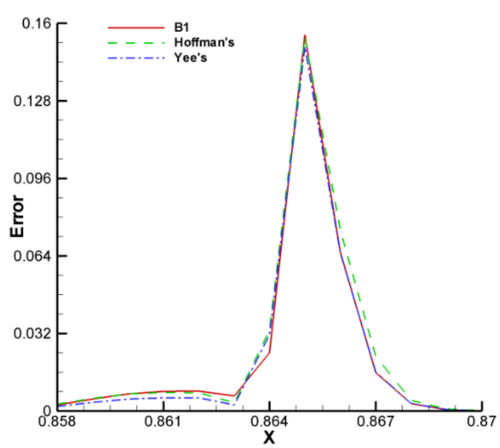

Fig 12: Error analysis for shock in case of Inverse Shock with B_1

It is observed that the hybridized scaling factors take the effect of first eigenvector (associated to the eigenvalue $u - c$) for expansion fan and the effect of third eigenvector (associated to the eigenvalue $u + c$) for shock region. Since both scaling factors β_1 and β_3 appearing in B_1 are non-constant therefore the impact of these factors vary case to case.

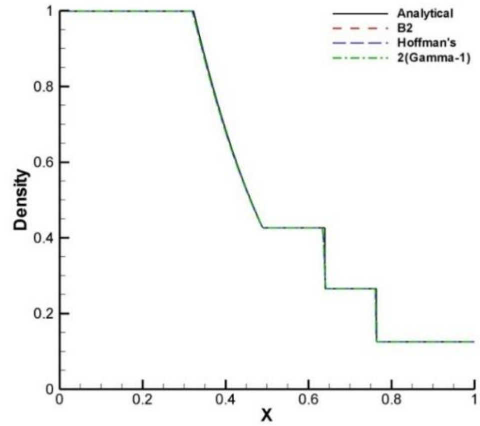

Fig 13: Density for SOD case with B_2

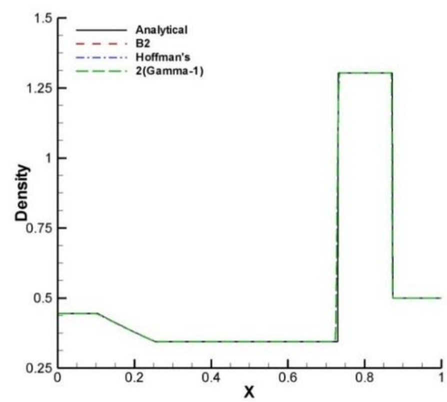

Fig 14: Density for Lax case with B_2

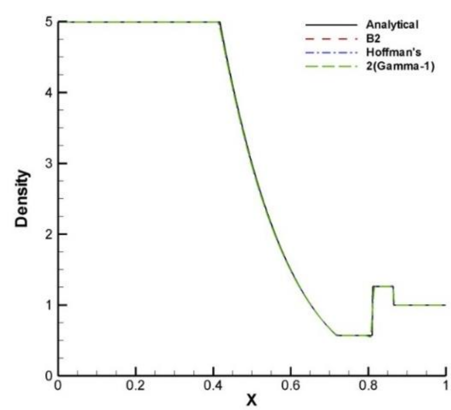

Fig 15: Density for Inverse Shock case with B_2

B. Behavior of TVD scheme with $\boldsymbol{B_2}$

The hybridization of scaling factor B_2 is performed by using Hoffman's scaling factor (β_1 in B_2) for the characteristic field which is more likely to affect the region of expansion fan and a normalizing factor (β_3 in B_2) for the characteristic field influencing the shock region and its neighborhood. Fig 13 to 15 represents the comparison of density profile for case of SOD, Lax and Inverse Shock boundary conditions respectively with B_2, Hoffman's suggested scaling and a new constant scaling factor introduced in this paper (β_3 in

B_2). In case of SOD, B_2 is approximately 2% more accurate than its individual components for expansion fan and contact whereas β_1 is leading in shock region as shown in Fig.16.

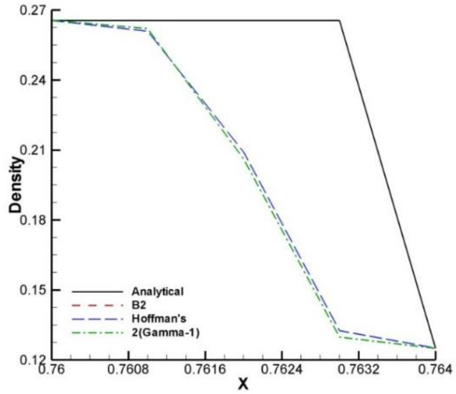

Fig 16: Shock for SOD case with B_2

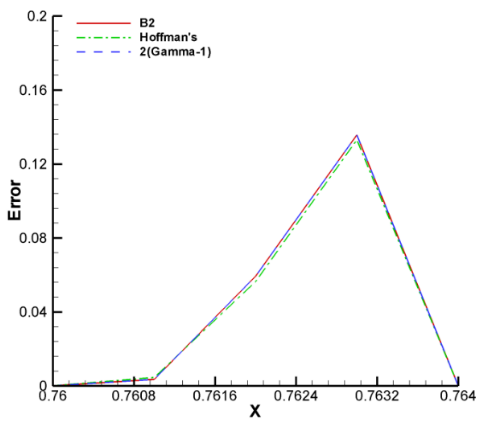

Fig 17: Error analysis for shock in case of SOD with B_2

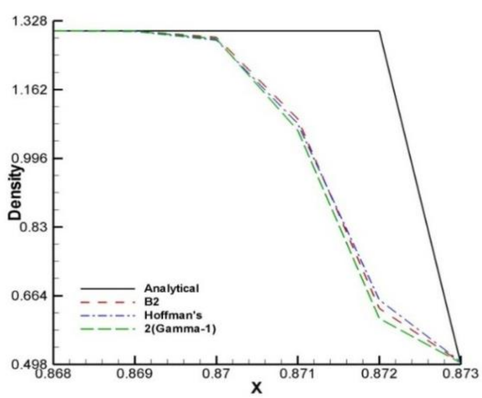

Fig 18: Shock for Lax case with B_2

The error estimation for shock location as shown in Fig 17 reveals that numerical dissipation is reduced by 3% on average with β_1, whereas B_2 and β_3 are found to be equally dissipative. For Lax case, B_2 is less accurate than β_1 in the region of contact discontinuity but results for expansion and shock are superior with B_2.

Fig 18 and 19 represent shock region and corresponding residuals for Lax test case. Similar behavior is observed in case of Inverse Shock with the exemption that β_3 in B_2 is more accurate across the shock as shown in Fig 20. Error analysis for shock location presented in Fig 21 depicts the accuracy of β_3 whereas, B_2 is still improved than β_1.

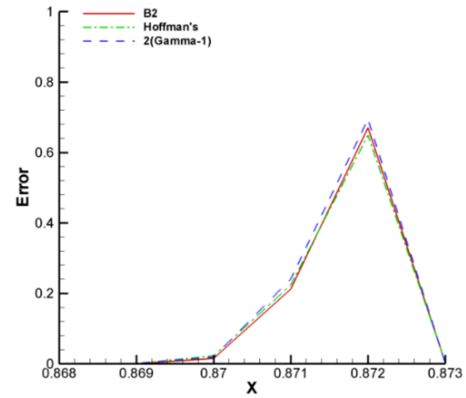

Fig 19: Error analysis for shock in case of Lax with B_2

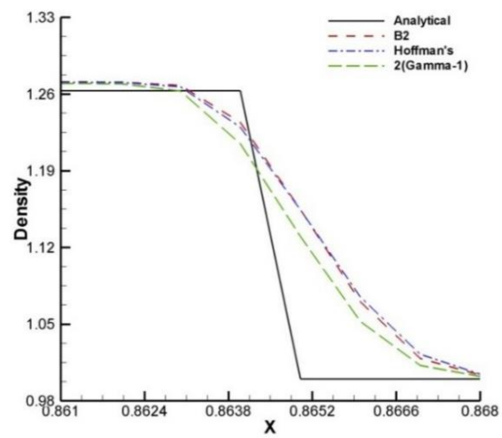

Fig.20 Shock for Inverse Shock case with B_2

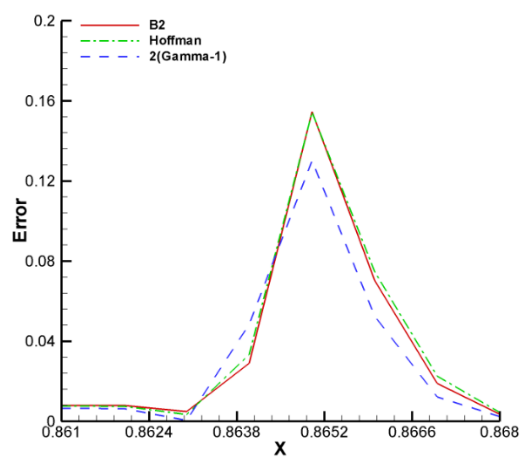

Fig.21 Error analysis for shock in case of Inverse Shock with B_2

It is observed that the normalizing constant (β_3 in B_2) used for scaling the eigenvector associated to eigenvalue $u + c$ proved to be good to capture shock precisely in two out of three test cases. This issue can be studied further for making it more general to be applicable in all cases in order to get desired results.

IV. Conclusion

Accuracy of numerical results is degraded due to false numerical dissipation near discontinuities in high speed flows. Hybridization of previously notable scaling factors for decoupling of hyperbolic conservation laws are proposed to encounter this issue. One of the scaling factors is formed by using the combination of Hoffman's and Yee's proposed scaling factors, whereas the second one is generated by Hoffman's scaling factor and normalizing constant of eigenvector matrix. The impact of proposed scaling on the behavior of Harten's 2nd order explicit TVD scheme is investigated by solving 1D shock tube problem subject to SOD, Lax and Inverse Shock boundary conditions. It is found that hybridized scaling factor which is composed of Hoffman's and Yee's scaling factors improved the results approximately 2% for expansion fan but its performance is not preferable over Hoffman's scaling factor for shock region in two out of three test cases, even so both are equally dissipative for contact discontinuity. Computed results with the scaling factor formed by combining Hoffman's scaling and normalizing constant are somewhat satisfactory in comparison for boundary conditions used in present study. However, contact discontinuity in case of Lax and shock region for SOD still have some margin of refinement for this scaling factor to be the best choice in reducing numerical dissipation.

The idea is based on treating each characteristic field according to their nature with dissimilar scaling factors. Despite all discrepancies, the concept of such hybridization has given new direction in the area of optimized decoupling of hyperbolic conservation laws, which can be explored further in 2D and 3D problems involving high speed flow physics.

References

[1] Harten, "On a Class of High-Resolution Total-Variation-Stable Finite Difference Schemes," SIAM Journal of Numerical Analysis, vol. 21, 1984.

[2] M. Hussain and C. H. Lee, "Comparative Study of Modern Shock Capturing Schemes," in Proceedings of Seventh ICFP, China, 2009.

[3] G. Peng-fei, W. hua-fei, C. Xiao, "Study on the Effects of Atmospheric Parameters on Space Vehicle Design," IOP Conference Series: Material Science and Engineering, vol. 608, 3rd International Conference on Aeronautical Materials and Aerospace Engineering, 2019.

[4] A. Harten, "High Resolution Schemes for Hyperbolic Conservation Laws," Journal of Computational Physics, vol. 49, no. 3, pp. 357-393, 1983.

[5] A. Harten and H. C. Yee, "Implicit TVD Schemes for Hyperbolic Conservation Laws in Curvilinear Coordinates," AIAA, vol. 25, no. 2, pp. 266-274(9), 1985.

[6] R.K. Dubey, "Flux Limited Schemes: Their Classification and Accuracy based on Total Variation Stability Regions," Applied Mathematics and Computations, pp. 325-336, 2013.

[7] D. Zhang, C. Jiang, D. Liang and L. Cheng, "A Review on TVD Schemes and a Refined Flux-Limiter for Steady-State Calculations," Journal of Computational Physics, vol. 302, pp. 114-154, 2015.

[8] S. Rathan, and G. N. Raju, "A Modified Fifth-Order WENO Scheme for Hyperbolic Conservation Laws," Computer & Mathematics with Applications, vol. 75, no. 5, pp. 1531-1549, 2018.

[9] K. A. Hoffmann, Computational Fluid Dynamics, 4 ed., vol. 2, Engineering Education System, 2000.

[10] H. Yee, "High Resolution Shock Capturing Schemes for Inviscid Viscous Hypersonic Flows," Journal of Computational Physics, vol. 88, no. 1, pp. 31-61, 1990.

[11] P. E. F. Toro, Riemann Solvers and Numerical Methods for Fluid Dynamics, A Practical Introduction, 3 ed., London: Springer Dordrecht Heidelberg London New York, 2009.

[12] H. C. Yee, R. Warming and A. Harten, "Implicit Total Variation Diminishing (TVD) Schemes for Steady-State Calculations," Journal of Computational Physics, vol. 57, no. 3, pp. 327-360, 1985.

[13] A. Harten and J. M. Hyman, "Self-Adjusting Grid Methods for One-Dimensional Hyperbolic Conservation Laws," Journal of Computational Physics, vol. 50, no. 2, pp. 235-269, 1983.

[14] H. C. Yee and J. L. Shinn, "Semi-Implicit and Fully Implicit Shock Capturing Methods for Hyperbolic Conservation Laws with Stiff Source Terms," in Eighth Computational Fluid Dynamics Conference, Honolulu, 1986.

[15] H. C. Yee, "A Class of High Resolution Explicit and Implicit Shock-Capturing Methods," NASA, California, 1989.

[16] M. Vinokur and H. C. Yee, "Extension of Efficient Low Dissipative High Order Schemes for 3-D Curvilinear Moving Grids," Frontiers of Computational Fluid Dynamics, pp. 129-164, 2002.

[17] Siddiqui, N.F and Hussain, M, "Decoupling of Hyperbolic Conservation Laws using an Improved Eigenvector Matrix," Journal of Mechanical Science and Technology, vol. 34, no. 3, pp. 1185-1193, 2020.